HHS Public Access

Author manuscript

Nat Immunol. Author manuscript; available in PMC 2014 July 01.

Published in final edited form as:

Nat Immunol. 2014 January ; 15(1): 63–71. doi:10.1038/ni.2766.

GEF-H1 controls microtubule-dependent sensing of nucleic acids for antiviral host defenses

Hao-Sen Chiang[#1], **Yun Zhao**[#1], **Joo-Hye Song**[1], **Song Liu**[1], **Ninghai Wang**[2], **Cox Terhorst**[2], **Arlene H. Sharpe**[3], **Megha Basavappa**[1], **Kate L. Jeffrey**[1], and **Hans-Christian Reinecker**[1]

[1]Gastrointestinal Unit and Center for the Study of Inflammatory Bowel Disease, Massachusetts General Hospital, Harvard Medical School

[2]Division of Immunology, Beth Israel Deaconess Medical Center and Center for the Study of Inflammatory Bowel Disease, Harvard Medical School

[3]Department of Microbiology, Harvard Medical School, Boston, Massachusetts 02114, USA

[#] These authors contributed equally to this work.

Abstract

Detailed understanding of the signaling intermediates that confer the sensing of intracellular viral nucleic acids for induction of type I interferons is critical for strategies to curtail viral mechanisms that impede innate immune defenses. Here we show that the activation of the microtubule-associated guanine nucleotide exchange factor GEF-H1, encoded by *Arhgef2*, is essential for sensing of foreign RNA by RIG-I-like receptors. Activation of GEF-H1 controls RIG-I and Mda5-dependent phosphorylation of IRF3 and induction of interferon-β expression in macrophages. Generation of *Arhgef2*$^{-/-}$ mice revealed a pronounced signaling defect that prevented antiviral host responses to encephalomyocarditis virus and influenza A virus. Microtubule networks sequester GEF-H1 that upon activation is released to enable antiviral signaling by intracellular nucleic acid detection pathways.

The induction of type I interferon (IFN) and activation of IFN-inducible genes are central to innate immune defenses against viral infection[1]. Intracellular sensors for microbial nucleic acids initiate complex signaling cascades that lead to the induction of proinflammatory cytokines and type I IFN for antiviral innate immune responses and the development of adaptive immunity[2].

Corresponding author: Hans-Christian Reinecker, M.D., Massachusetts General Hospital 55 Fruit Street GRJ 711, Boston Massachusetts, USA 02114, Tel: 617-724-2172; Fax: 617-726-3673 hans-christian_reinecker@hms.havard.edu..

Note: Supplementary Information *is available in the online version of the paper*.

AUTHOR CONTRIBUTIONS

HSC, YZ, JHS, SL, NW, and MB carried out experiments; KJ, AHS and CT supported the development of research tools and mice; KJ provided virus and advised on virus infection experiments; HCR conceived of, directed all research and along with HSC, prepared the manuscript.

COMPETING FINICIAL INTERESTS

The authors declare no competing financial interests.

Viral targeting of dynein-based transport mechanisms play an important role for intracellular movements and replication of viral pathogens[3], although it is unresolved how microtubule-based trafficking of signaling components contributes to the induction of antiviral defenses. GEF-H1, also called lfc in mice, was originally identified as a member of the Dbl family that is sequestered on microtubules and directs spatio-temporal activation of Rho GTPases[4]. Inactive GEF-H1 binds to the dynein motor complex on microtubules[5]. GEF-H1 can be activated and released from microtubules upon cellular interactions with bacterial effectors[6,7] and subsequently contributes to intracellular pathogen recognition[7,8].

The innate immune system senses viral infection through cytosolic and transmembrane receptors leading to activation of cell type-specific regulatory networks that activate IFN regulatory factors (IRFs) and NF-κB for the induction of type I interferons and proinflammatory cytokines. IFN-β expression is initially induced after viral RNA binding to Toll-like receptors (TLRs) that signal through MyD88 and TRIF[9]. Single stranded viral RNA (ssRNA) can be detected by TLR7 in endosomes[10]. Double-stranded viral RNA (dsRNA) can be recognized by endosomal TLR3[11]. In addition cell surface TLRs such as TLR4 and TLR2 are activated by viral glycoproteins[12].

During viral replication several members of the DExD/H-box helicases (DDX) protein family comprised of RNA and DNA helicases function as viral RNA and DNA sensors[13,14]. The CARD domain-containing DDX proteins, retinoic acid-inducible gene I (RIG-I) and melanoma differentiation-associated gene 5 (Mda5), also recognized as RIG-I-like receptors (RLR), are important inducers of innate immunity and recognize complementary variants of viral RNA to distinguish between virus families[15,16]. Mda5 is required for type I IFN responses to long cytoplasmic viral and synthetic dsRNA and is activated by picornavirus[1517], whereas RIG-I recognizes short blunt or 5′-triphosphorylated ends of viral genomic RNA segments and is required for defense activation against influenza, paramyxovirus and rhabdovirus families[16,17,18,19]. RIG-I and Mda5 signal transduction requires mitochondrial antiviral signaling protein (MAVS), also called IFN-β promoter stimulator 1 (IPS-1), for the activation of TBK1 (TANK [TRAF (tumour necrosis factor receptor-associated factor) family member-associated nuclear factor κB activator]-binding kinase 1) and IKKε that mediate the phosphorylation of IRF3 for the induction of type I IFNs[20]. TBK1 and IRF3 activation also occurs downstream of stimulator of interferon genes (STING; also known as TMEM173, MPYS, ERIS or MITA), in the detection of viral nucleic acids and B-form DNA (B-DNA or poly(dA:dT)) by DDX proteins)[21].

Here we demonstrate that GEF-H1 mediates the induction of antiviral host defenses by cytosolic receptors RIG-I and Mda5 in macrophages. The recognition of viral RNA and synthetic dsRNA in the MAVS pathway was dependent on microtubule networks that were required for the activation and interaction of GEF-H1 with TBK1-IKKε for the induction of IRF3 phosphorylation and subsequent induction of *Ifnb1* gene expression. In contrast, deletion of GEF-H1 or disruption of microtubule function in macrophages still allowed NF-κB activation by cell surface and endosomal TLR activation. Consequently, GEF-H1 was required for the restriction of ssRNA virus replication and the induction of antiviral host defense against EMCV and influenza A.

RESULTS

GEF-H1 controls RLR signaling

To define the role of GEF-H1 in innate immune activation by foreign nucleic acids, we generated GEF-H1-deficient mice using C57BL/6 embryonic stem cells with a gene-trap insertion between exons 4 and 5 of *Arhgef2* on mouse chromosome 3 that prevents GFH-H1 mRNA (Fig. 1a) and protein expression (Fig. 1b). These mice had normal T cell, B cell and mononuclear phagocyte numbers in spleen and lymph nodes (Supplementary Fig. 1).

IFN-β protein secretion and mRNA expression were determined in response to 1-8 kb (high molecular weight, HMW) polyriboinosinic:polyribocytidylic acid (poly(I:C)) as a ligand for Mda5 or 0.3-1.2 kb (low molecular weight, LMW) poly(I:C) and 5′-triphosphate (5′ppp)-double-stranded (ds)RNA were used as synthetic ligands for RIG-I[18]. In addition, cyclic diguanosine monophosphate (c-di-GMP) was used as a DDX41 ligand that induces STING-dependent IFN-β expression[22]. Expression of *Ifnb1* mRNA was significantly reduced in bone marrow-derived macrophages derived from GEF-H1-deficient mice in response to MAVS and STING-mediated recognition of nucleic acids (Fig. 1c). In contrast, GEF-H1-deficient macrophages upregulated *Ifnb1* mRNA expression in response to TLR1/2, TLR2, TLR4, TLR5, TLR2/6, TLR7 and TLR9 activation by specific ligands comparable to wild-type macrophages (Fig. 1d).

The lack of transcriptional activation of *Ifnb1* upon RIG-I activation by 5′ppp-dsRNA resulted in significantly less IFN-β secretion in GEF-H1-deficient macrophages compared to wild-type macrophages (Fig. 1e). GEF-H1-deficient macrophages also secreted significantly less IFN-β after transfection of HMW and LMW poly(I:C) (Fig. 1f), and even demonstrated significantly attenuated IFN-β secretion when HMW poly(I:C) was directly added to the culture medium (Fig. 1g). Furthermore, GEF-H1 expression itself was upregulated by RIG-I signaling initiated by 5′ppp-dsRNA transfection into macrophages (Fig. 1h). Remarkably, two intact alleles of *Arhgef2* were required to induce a full response to poly(I:C), since macrophages heterozygous for gene-trap insertion also demonstrated impaired *Ifnb1* mRNA expression (Fig. 1i). GEF-H1-deficient macrophages also demonstrated reduced *Il6* and *Tnf* mRNA expression in response to 5′ppp-dsRNA, indicating a profound innate signaling defect in the activation of MAVS-dependent RLR signaling (Fig. 1j). In contrast, TRIF- and MyD88-mediated induction of IFN-β secretion and *Il6* and *Tnf* mRNA expression were not reduced in GEF-H1-deficient macrophages in response to the TLR4 ligand lipopolysaccharide (LPS) (Supplementary Fig. 2).

The RLR signaling deficiency in GEF-H1-deficient macrophages was not due to impaired poly(I:C) uptake. HMW rhodamine-labeled poly(I:C) was similarly absorbed from the medium in GEF-H1-deficient and wild-type macrophages and found in association with vesicular and tubular compartments in wild-type and GEF-H1-deficient macrophages (Supplementary Fig. 3a,b). Together these data indicated that GEF-H1 expression is induced by foreign intracellular dsRNA and required for the signaling of intracellular nucleotide sensors leading to IFN-β secretion and proinflammatory cytokine expression in macrophages.

GEF-H1 regulates MAVS-dependent activation of IRF3

RLRs-induced type I IFN gene transcription requires MAVS and TBK1-IKKε and is mediated primarily through IRF3[23]. IRF3 is localized in the cytoplasm and, upon stimulation, becomes activated by serine/threonine phosphorylation leading to nuclear translocation and binding to recognition sequences in the promoters and enhancers of type I IFNs[20]. To determine whether GEF-H1-dependent type I interferon induction was mediated by IRF3 phosphorylation and nuclear translocation in response to RLR activation, we stimulated GEF-H1-deficient and wild-type macrophages with the RIG-I ligand 5′ppp-dsRNA and analyzed the resulting phosphorylation of IRF3 in cell lysates as well as nuclear translocation of IRF3. Phosphorylation of IRF3 in response to RIG-I activation was significantly reduced in GEF-H1-deficient macrophages when compared to wild-type macrophages (Fig. 2a). IRF3 remained undetectable 4 h after 5′ppp-dsRNA stimulation in the nuclei of GEF-H1-deficient macrophages, demonstrating a profound deficiency in IRF3 activation (Fig. 2b). In contrast, IRF3 phosphorylation in response to LPS occurred at much lower amounts in bone marrow-derived macrophages under same conditions but was detectable similarly in wild-type and GEF-H1-deficient macrophages (Fig. 2c).

We further found that the RIG-I ligand 5′ppp-dsRNA and Mda5 ligand HMW poly(I:C) induced p65 phosphorylation and IκBα degradation in GEF-H1-deficient and wild-type macrophages over a period of 4 h (Fig. 2d). Both, GEF-H1-deficient and wild-type macrophages also responded within 15 minutes with comparable NF-κB activation to TLR4 activation (Fig. 2d). This data indicated that GEF-H1 function was required for IRF3 activation in the RLR pathway but dispensable for p65 activation in the TLR4 and RLR pathways.

Furthermore, GEF-H1-deficient macrophages showed significantly less *Ifnb1* promoter activation in response to MAVS expression compared to wild-type macrophages while GEF-H1 expression enhanced *Ifnb1* promoter activation in wild-type macrophages and complemented MAVS-induced IFN-β responses in GEF-H1-deficient macrophages (Fig. 2e).

We further found that GEF-H1 enhanced MAVS signaling leading to the activation of a p561 interferon-stimulated response element (ISRE)-containing promoter that is activated by IRF3, but not NF-κB[24] (Fig. 2f). GEF-H1 increased ISRE-induced transcriptional activity 10-fold compared to MAVS expression alone in HEK293T cells (Fig. 2f). Indeed, GEF-H1 augmented MAVS-dependent phosphorylation of endogenous IRF3 in HEK293T cells without significantly altering the baseline expression of IRF3 or TBK1 (Fig. 2g).

To further characterize the role of GEF-H1 in signaling of intracellular nucleotide receptors and induction of *Ifnb1* promoter activation, we utilized HEK293T cells that lack TLR3, TLR4, TLR7/8 and TLR9. We assembled Mda5 or RIG-I signaling pathways in HEK293T cells in the absence or presence of GEF-H1 to assess the activation of a luciferase reporter containing the *Ifnb1* promoter in response to RLR ligands. GEF-H1 expression significantly enhanced *Ifnb1* promoter activation induced by the expression of Mda5 and RIG-I alone and further enhanced Mda5-mediated detection of HMW poly(I:C) and RIG-I-dependent responses to LMW poly(I:C) and 5′ppp-dsRNA (Fig. 2h). In contrast to RIG-I and Mda5,

GEF-H1 expression in HEK293T cells did not induce *Ifnb1* promoter activation by itself or rendered HEK293T cells responsive to RLR stimulation when expressed alone (Fig. 2h). Together these data demonstrated that GEF-H1 functions in conjunction with RLRs, enhancing the detection of intracellular poly(I:C) and 5′ppp-dsRNA and leading to the activation of the *Ifnb1* promoter.

The phosphorylation, dimerization and nuclear translocation of IRF3 for the activation of IFN-β transcription require IKKε and TBK1[23]. Indeed, expression of either TBK1 or IKKε enhanced *Ifnb1* promoter activation in HEK293T cells (Fig. 2i). GEF-H1 expression significantly enhanced *Ifnb1* promoter activation by TBK1 alone or in conjunction with IKKε (Fig. 2i). In contrast, GEF-H1 did not augment TBK1 or IKKε mediated *Nfkb1* promoter activation (Fig. 2i). Furthermore, the promotion of IRF3 and *Ifnb1* gene promoter activation by GEF-H1 was dependent on functional TBK1 and therefore absent in the presences of a TBK1 kinase-inactive (K38A) mutant (Fig. 2j). Together these data demonstrate that GEF-H1 can function in the RLR pathway in conjunction with MAVS and TBK1/IKKε to enhance the phosphorylation of IRF3 and activation of the *Ifnb1* promoter.

GEF-H1 mediates microtubule-dependent RLR signaling

To better define the functional domains of GEF-H1, we created GEF-H1 variants by exchanging the tyrosine at position 393 with alanine to disable the GTP loading capacity of the Dbl homology domain (ΔDH)[25], by replacing serine 885 with alanine (S885A) to prevent phosphorylation that inhibits GEF activity of GEF-H1 or by substituting cysteine 53 with an arginine (C53R) in the n-terminal zinc finger domain that is required for association of GEF-H1 with microtubules[26,27]. We expressed GFP-tagged GEF-H1 or its active mutants GEF-H1 (S885A) and GEF-H1 (C53R) or its GEF-deficient mutants to determine subcellular localization and association with the microtubule network. Confocal microscopy revealed that GEF-H1 or GEF-H1 (S885A) induced the formation of microtubules that formed aggregations and long curved filaments that contained α-tubulin (Fig. 3a). GEF-H1 ΔDH was found in the cytoplasm and co-localized with microtubules, but failed to induce microtubule aggregations (Fig. 3a). GEF-H1 (C53R) was unable to bind microtubules and therefore was found expressed in the cytoplasm and in intracellular aggregations (Fig. 3a).

Both the microtubule associating active GEF-H1 (S885A) and the cytoplasmic GEF-H1 (C53R) mutants significantly enhanced MAVS signaling when expressed in HEK-293T cells (Fig. 3b). In contrast, we found that the DH domain of GEF-H1 was required for the amplification of MAVS-induced *Ifnb1* promoter activation (Fig. 3c). Furthermore, the ΔDH variant of GEF-H1 failed to enhance TBK1-mediated *Ifnb1* promoter activation; together indicating that IRF3 activation in the presence of GEF-H1 was dependent on nucleotide exchange activity by GEF-H1 (Fig. 3d). Indeed, MAVS-induced *Ifnb1* promoter activation was abrogated in the presence of a dominant negative RhoAT19N mutant (Fig. 3e).

Since GEF-H1 is sequestered on microtubules where its GEF function is inhibited by phosphorylation of S885[5], we hypothesized that activation of GEF-H1 by dephosphorylation and release from microtubules may be required for RLR signaling. Immunostaining with antibodies directed against α-tubulin or phalloidin staining revealed intact microtubule and actin networks in unstimulated and poly(I:C)-stimulated wild-type and GEF-H1-deficient

macrophages (Supplementary Fig. 3c,d). However, upon disruption of microtubules, macrophages failed to initiate *Ifnb1* transcription after poly(I:C) and 5′ppp-dsRNA stimulation (Fig. 3f), although nocodazole treatment of macrophages did not prevent the uptake of poly(I:C) into macrophages (Supplementary Fig. 3e). Nocodazole treatment also reduced STING-mediated *Ifnb1* mRNA expression in macrophages in response to c-di-GMP (Fig. 3g). The induction of TRIF-dependent IFN-β expression upon TLR4 activation in macrophages remained unchanged in the presence of nocodazole and thus occurred independent of the microtubule formation in macrophages (Fig. 3f).

We further found that a functional microtubule network was required for the interaction of GEF-H1 with TBK1 because GEF-H1-containing complexes lacked TBK1 in the presence of nocodazole, while neither TBK1 nor GEF-H1 expression was impaired under these conditions (Fig. 4a,b).

TBK1-containing signaling complexes preferably contained GEF-H1 that was dephosphorylated at S885 (Fig. 4c). Potential protein phosphatases that are associated with microtubule function, activated by foreign RNA and targeted by viral mediators include protein phosphatase 2A (PP2A)[28]. Inhibition of PP2A for 40 minutes using 1 nM okadaic acid, enhanced S885 phosphorylation of GEF-H1, but reduced its association with TBK1-containing signaling complexes (Fig. 4c,d). We also found reduced GEF-H1 in association with TBK1 after addition of forskolin (Fig. 4c), to stimulate the activation of adenylyl cyclase, increasing cellular concentrations of cAMP and subsequent S885 phosphorylation of GEF-H1 by protein kinase A (PKA)[26] (Fig. 4d).

Functionally, GEF-H1 phosphorylation by forskolin or okadaic acid prevented the induction of IFN-β in macrophages by poly(I:C) but failed to impede *Ifnb1* expression in response to LPS (Fig. 4e). Furthermore, GEF-H1 was dephosphorylated when the RLR signaling pathway was activated by infecting COS-7 cells with NS1-deficient Influenza A (A/PR/8/34 ΔNS1) (Fig. 4f).

In aggregate, these data are consistent with a multistep activation and release of GEF-H1 from microtubules to make its GEF activity available for amplification of RLR-mediated activation of TBK1-IKKε-dependent *Ifnb1* promoter activation.

GEF-H1 functions in ssRNA virus detection

Thus far our data indicated that GEF-H1 regulates MAVS-dependent utilization of TBK1 for IRF3 phosphorylation and nuclear translocation for type I IFN induction. Furthermore, macrophages derived from *Arhgef2*$^{-/-}$ mice were impaired in response to 5′ppp-dsRNA and poly(I:C) stimulation but responded to TLR activation with type I IFN secretion, indicating that GEF-H1 functions in the RIG-I and Mda5-dependent induction of type I IFNs for antiviral defense.

We next assessed susceptibility of GEF-H1-deficient macrophages to distinct RNA viruses that activate the innate immune system to varying degree through RLRs and TLRs and compared the innate immune responses to those elicited in MAVS-deficient macrophages. Encephalomyocarditis virus (EMCV) is a positive-sense ssRNA virus of the Picornaviridae

that is primarily detected by Mda5-dependent host responses[16]. GEF-H1-deficient macrophages were severely impaired in their ability to respond to EMCV infection with IFN-β secretion compared to wild-type macrophages when infected at the multiplicity of infection (MOI) of 0.1 (Fig. 5a). The reduction in IFN-β secretion was similarly observed in MAVS-deficient macrophages upon infection with EMCV (Fig. 5a). This effect was likely due to reduced IRF3 phosphorylation in the absence of GEF-H1 (Fig. 5b), since NF-κB activation was similar in GEF-H1-deficient, MAVS-deficient and wild-type macrophages 16 h after EMCV infection (Fig. 5c). As a consequence of reduced IFN-β secretion, virus replication was enhanced in GEF-H1-deficient macrophages as indicated by the significantly increased expression of transcripts encoding for EMCV non-structural protein 2A and 2B (Fig. 5d). Together, these experiments indicated that GEF-H1, MAVS and Mda5 are similarly required for host defense activation to EMCV.

Influenza A (Puerto Rico 8/1934 strain, PR/8/1934), is recognized by RIG-I[16] and DHX9[29]. However, TLR7 contributes to type I interferon secretion by plasmacytoid dendritic cells to the virus Influenza A[30]. We assessed IFN-β expression in GEF-H1-deficient macrophages after infection with a non-structural protein (NS)1-deficient influenza A variant[31], that is unable to inhibit host IFN-β responses during viral replication. GEF-H1-deficient macrophages lacked nuclear translocation of IRF3 in response to NS1-deficient influenza A infection (Fig. 5e), although the cytoplasmic amounts of IRF3 were comparable to wild-type macrophages (Fig. 5f). Consequently, GEF-H1-deficient macrophages secreted significantly less IFN-β at 8 and 12 h after infection compared to wild-type macrophages (Fig. 5g). The reduction in IFN-β secretion was similarly observed in MAVS-deficient macrophages upon infection with NS1-deficient influenza A (Fig. 5g). However, NF-κB activation in response to NS1-deficient influenza A infection was independent of GEF-H1 and MAVS in macrophages (Fig. 5h). This suggested that alternative pathways contribute to IFN-β secretion in response to Influenza A infection that are not impaired in either GEF-H1 or MAVS-deficient macrophages. Despite reduced IFN-β expression, GEF-H1-deficient macrophages demonstrated increased expression of Influenza A nucleoprotein (NP) indicating enhanced viral replication compared to wild-type macrophages (Fig. 5i). Even when we infected NS1-sufficient influenza A, *Ifnb1* mRNA induction was significantly reduced in GEF-H1-deficient macrophages 12 and 24 h after infection (Fig. 5j). Moreover, viral replication was enhanced as measured by NS1 RNA expression and the replication of a recombinant influenza virus carrying a GFP reporter gene in the NS segment[32] in GEF-H1-deficient macrophages (Fig. 5k and Supplementary Fig. 4a).

Vesicular stomatitis virus (VSV) is a negative single stranded rhabdovirus that activates IFN-α/β through RIG-I, but not protein kinase R (PKR), Mda5 or TLR3[16,33]. However, glycoprotein G of VSV is a ligand for TLR4 and can trigger IFN-α/β production independent of RIG-I[33]. At a functional level TLR4 and MAVS or RIG-I-dependent type I IFN production appear non redundant since both MAVS-deficient mice and TLR4 mutant mice are highly susceptibility to VSV[33,34]. We found that GEF-H1-deficient macrophages were impaired in the ability to restrict VSV replication (Supplementary Fig. 4b-d). In these experiments, we infected macrophages from *Arhgef2*$^{-/-}$ mice and wild-type littermates with an MOI of 0.1 with VSV and followed virus production in the supernatants over two days by

infecting BHK cells. Beginning 4 h after infection, GEF-H1-deficient BMDMs produced 0.8-1.3 log phase higher amounts of active virus for 24 h compared to wild-type macrophages (Supplementary Fig. 4b). However, VSV infection of GEF-H1 or MAVS-deficient macrophages induced IFN-β at similar amounts to infected macrophages with intact *Arhgef2* loci 12 to 48 h after infection. (Supplementary Fig. 4c and d). This is consistent with the finding that TLR4 signaling leading to IFN-β expression remained intact in GEF-H1-deficient macrophages and indicated that GEF-H1 selectively controlled RLR-dependent antiviral defense.

GEF-H1 functioned in mediating RLR recognition of viral RNA rather than by mediating type I interferon signaling, since IFN-α/β receptor activation leading to the phosphorylation of STAT1 was intact in GEF-H1-deficient macrophages (Supplementary Fig. 4e).

Finally, we determined innate host defense responses in GEF-H1-deficient macrophages to *Salmonella typhimurium*. The recognition of *S. typhimurium* is for the most part mediated by TLR2, TLR4 and TLR5 when cultured under conditions that favor *Salmonella* pathogenicity island 2 (SPI-2) expression[35]. GEF-H1-deficient macrophages expressed comparable *Ifnb1* and *Tnf* mRNA levels to wild-type macrophages after infection with *S. typhimurium* **(**Supplementary Fig. 5a, b**)**. Further, absence of GEF-H1 expression did not protect macrophages from invasion and intracellular replication of *S. typhimurium* (Supplementary Fig. 5c). Together these data demonstrate that GEF-H1 facilitates RIG-I and Mda5-dependent host defenses to viral pathogens without preventing the activation of IFN-α/β or TLR receptor signaling in macrophages.

Host defense against influenza requires GEF-H1

We next assessed the susceptibility of *Arhgef2*$^{-/-}$ mice to influenza A infection to determine whether GEF-H1 was required for antiviral innate immune responses *in vivo*. We first determined whether alveolar macrophages of GEF-H1-deficient mice were impaired in recognizing poly(I:C). Bronchoalveolar fluid from GEF-H1-deficient mice lacked detectable IFN-β when challenged intranasally with poly (I:C), whereas wild-type mice secreted significant amounts of IFN-β in the airways in response to the same challenge (Fig. 6a). We also isolated alveolar macrophages and examined the concentration of IFN-β secretion after the initial intranasal challenge with poly(I:C) *in vivo* and assessed their responsiveness to additional challenges with poly(I:C). While alveolar macrophages from wild-type littermates significantly increased IFN-β secretion upon re-stimulation *in vitro*, no detectable IFN-β was released from GEF-H1-deficient alveolar macrophages after isolation or following re-stimulation *in vitro* suggesting a severe defect in the recognition of poly(I:C) by alveolar macrophages which we hypothesized would impair viral defense in these mice (Fig. 6b).

Indeed, GEF-H1-deficient mice were more susceptible to Influenza A infection compared to wild-type littermates. Four days after Influenza A infection, alveolar macrophages from GEF-H1-deficient mice expressed significantly lower levels of *Ifnb1* and *Il6* mRNA (Fig. 6c). Additionally, lungs of GEF-H1-deficient mice demonstrated significantly more signs of severe inflammation, with increased epithelial damage, mononuclear cell infiltrates, and alveolitis (Fig. 6d). This suggests that GEF-H1 is required for IFN-β induction for antiviral responses against influenza A infection.

DISCUSSION

GEF-H1-deficient macrophages have a profound defect in the induction of IFN-β following detection of synthetic dsRNAs including HMW and LMW poly(I:C) and 5′ppp-dsRNA. The inability to induce IFN-β in the absence of GEF-H1 was not due to impaired uptake of ligands or differential expression of signaling intermediates, but the requirement of the nucleotide exchange activity of GEF-H1 and polarized microtubules for RLR signaling. In macrophages GEF-H1 is dephosphorylated and released from microtubules during RLR activation and promotes IRF3 activation. Disruption of microtubule polarization prevents activation of GEF-H1 and consequently RLR signaling. Remarkably, TRIF and MyD88 dependent activation of IFN-β and proinflammatory cytokine expression was neither dependent on GEF-H1 nor nocodazole sensitive microtubule formation, suggesting that GEF-H1 has a distinct spatial function that is required for the activation of TBK1-IKKε in the RLR pathway (Supplementary Fig. 6).

Viral pathogens often target dynein machinery components with effectors to utilize the microtubule system for transport in host cells[3]. GEF-H1 may serve as gatekeeper on microtubules to locally modulate the activity of GTPases that in turn are responsible for the initial polarization of the microtubule cytoskeleton to facilitate antiviral responses[36]. Recently the microtubule network has been demonstrated to mediate the aggregation of mitochondria to facilitate the activity of the NLRP3 inflammasome[37]. Rho GTPase activation by GEF-H1 may stabilize actin association with mitochondria that occurs during RIG-I signaling during influenza A infection of macrophages[38]. In this context, GEF-H1 could regulate local Rho GTPase activation to promote stabilizing microtubules[39] or membrane compartments as signaling platforms that allow GEF-H1 to interact with TBK1-IKKε containing signaling complexes. Furthermore, GEF-H1 may regulate the distribution of mitochondria within cells that requires crosstalk between microtubule and actin cytoskeleton through Rho GTPase activation[40].

GEF-H1 and MAVS-deficient macrophages were impaired in RLR signaling leading to IRF3 activation. In contrast, NF-κB activation by surface and endosomal TLRs involved in the detection of viral RNA and viral glycoprotein remained intact in GEF-H1-as well as MAVS-deficient mice. Although TRIF-dependent TLR signaling can activate TBK1[41] and IRF3 activation[42], we showed that in macrophages LPS stimulation induced primarily NF-κB activation. This is consistent with the finding that TLR-dependent NF-κB activation can occur independent of TBK1[41] but still can control IFN-β expression[43] since the IFN-β promoter contains IRF3 and NF-κB sites that are utilized for induction by different signaling pathways[44]. Conversely, NF-κB is dispensable for IFN-β activation by RLRs that is mediated by IRF3 activation[45,46].

GEF-H1 was not required for IFN-β secretion initiated by ligand binding to TLR1/2, TLR2, TLR2/6, TLR4, TLR5, TLR7 and TLR9 activation in macrophages. In addition, the induction of proinflammatory cytokines by TLR4 activation, which requires both MyD88- and TRIF-dependent signals[47], was intact in GEF-H1-deficient macrophages. We further demonstrate that innate immune responses to viruses whose RNA or glycoptroteins also activates TLRs or invasive bacteria that activate TLRs were able to induce IFN-β expression

even in the absence of GEF-H1 or MAVS. However the current experiments do not exclude a further function of GEF-H1 in TLR signaling in different cell types or in response to distinct pathogens that have different effector functions to evade host detection.

Our experiments demonstrate that GEF-H1-deficient macrophages fail to activate IRF3 but not NF-κB in response to ssRNA viruses. Because both IRF3 and NF-κB activate IFN-β, the role of GEF-H1 may depend on the degree to which antiviral host response to a particular pathogen includes the activation of RLR and TLR pathways. GEF-H1- and MAVS-deficient macrophages responded similarly to infection with EMCV with a profound lack of IFN-β secretion. Thus GEF-H1 is required for the recognition of EMCV infection that primarily occurs through Mda5[15,16]. Mda5 is required and dominant over TLR3 for type I IFN induction by uncomplexed poly(I:C) in bone marrow-derived macrophages and DCs *in vitro*[15] and we therefore cannot exclude a role of GEF-H1 in TLR3 signaling in different cell types.

GEF-H1- as well as MAVS-deficient macrophages demonstrate a significant reduction in IFN-β secretion in response to influenza A infection. In conventional dendritic cells and macrophages, RIG-I is required for the detection of influenza virus and induction of type I IFN via recognition of 5′-triphosphates on genomic ssRNA, which are generated after viral fusion and replication[19]. Our data demonstrate RIG-I activation in response to 5′ppp-dsRNA was impaired in GEF-H1-deficient macrophages resulting in attenuation of IRF3 phosphorylation, nuclear translocation and *Ifnb1* gene transcription. Furthermore, GEF-H1-deficient alveolar macrophages failed to respond directly to stimulation or re-stimulation with poly(I:C) with IFN-β secretion. GEF-H1 was essential for host response to Influenza A, which was pronounced during infection with an NS1-deficient influenza A variant that lacks the ability of the wild-type virus to inhibit type I IFN secretion. It will be important to determine whether NS1 targets GEF-H1 function in host cells for immune evasion since variants of NS1 can regulate viral RNA load and RIG-I-mediated innate immune activation through mechanisms that may include targeting Rho GTPase function but have not been fully established[48].

Our data indicate that GEF-H1 and polarization of microtubules are also required for the recognition of c-di-GMP that induces STING-mediated activation of TBK1 and IRF3[22]. c-di-GMP serves as an important non-coding RNA binding second messenger in bacteria regulating the expression of many virulence genes[49]. Through binding to DDX41 and STING, c-di-GMP is recognized as a pathogen-associated molecular pattern that triggers the host type I interferon innate immune response[22]. Thus the role of GEF-H1 in the activation of IRF3 may also mediate DDX protein functions for the induction of type I interferon responses to bacterial infections. It will be important to define the role of GEF-H1 in other STING-dependent recognition pathways that include a large number of proposed sensors for cytosolic DNA sensing whose role in antimicrobial immunity and viral defense activation is currently being investigated[50]

In conclusion, our findings identify GEF-H1 as an antiviral signaling component that directs utilization of TBK1-IKKε in the MAVS-dependent nucleic acid detection pathways for the sensing of ssRNA virus infection and induction of IFN-β expression and secretion. GEF-H1

therefore possesses a pivotal role in mounting defenses against non-self RNA through RLRs, and thus understanding of the underlying molecular mechanisms of GEF-H1 activation and release from microtubules could lead to new therapeutic strategies against viral infection.

ONLINE METHODS

Generation of *Arhgef2*$^{-/-}$ mice

Arhgef2$^{-/-}$ mice were generated using the gene-trap ES cell clone IST13976A8 for *Arhgef2* from the Texas Institute of Genomic Medicine (TIGM). ES cell clone were microinjected into C57BL/6 blastocysts. Chimeric offspring were used for the generation of homozygous mice for the targeted null allele (*Arhgef2*$^{-/-}$). Genotyping was performed by PCR of tail genomic DNA using two sets of primers: F139_1, 5′-agtcccctgtccagtggtttacc-3′ and R_V76, 5′-ccaataaaccctcttgcagttgc-3′; F_V76, 5′-cttgcaaaatggcgttacttaagc-3′ and R139_4, 5′-agactcagggtcactggttgtga-3′ to produce amplicons that span the gene-trap vector junction to distinguish the *Arhgef2*$^{-}$ allele from the *Arhgef2*$^{+}$ allele. PCR of tail genomic DNA was performed to distinguish the *Arhgef2*$^{+}$ allele from the *Arhgef2*$^{-}$ allele using the F139_1 and R139_4 primers to produce an amplicon that spans the gene-trap vector insertion site. GEF-H1 mRNA was confirmed by RT-PCR using a forward primer spanning from exon 4~5 junction, 5′-aggcaaccaagacccgggaaaa-3′ and a reverse primer located in exon 12, 5′-taaggccttggtgtggcggc-3′. GEF-H1 protein expression was confirmed by immunoblotting. Mice were housed in pathogen-free barrier facilities. *Arhgef2*$^{-/-}$ and littermate control mice were used throughout the experiments. All animal experiments were performed according to animal protocols approved by the Subcommittee on Research Animal Care at Massachusetts General Hospital. Unless otherwise indicated, experiments used sex-matched littermates at 8-12 weeks of age.

Cells and reagents

HEK293T and COS-7 cells were purchased from American Type Culture Collection and maintained in DMEM supplemented with 10% fetal bovine serum and 0.5% penicillin/streptomycin mixture and tested to be free of mycoplasma. Bone marrow-derived macrophages were generated in DMEM containing 10% FBS, 0.5% penicillin/streptomycin mixture, and 20 ng/ml M-CSF for 5-7 days. Control dsRNA, 5′ppp-dsRNA, LMW poly(I:C), HMW poly(I:C), LPS,c-di-GMP, Pam3CSK4, HKLM, Flagellin, FSL-1, ssRNA, and CpG ODN1826 were purchased from Invivogen. Nocodazole and gentamicin solution was obtained from Sigma. Forskolin and okadaic acid were purchased from Abcam.

Plasmids and antibodies

Plasmids encoding VSV-tagged GEF-H1, RhoA, RhoAT19N, and RhoAG14V have been described previously[7]. Plasmid encoding FLAG-tagged GEF-H1 (pCMV6-Entry-hGEF-H1) and GFP-tagged GEF-H1 (pCMV6-AC-GFP-hGEF-H1) were purchased from OriGene. FLAG-GEF-H1 (Y393A, ΔDH), GFP-GEF-H1 (Y393A, ΔDH), GFP-GEF-H1 (S885A), and GFP-GEF-H1 (C53R) mutations were generated using the Quikchange Site-Directed Mutagenesis Kit (Stratagene). pEF-BOS-huTBK1, pEF-BOS-huTBK1K38A, pcDNA3-IKKε-flag, pEF-BOS-huMAVS, pEF-BOS-huRIG-I and pEF-BOS-huMDA5 plasmids were obtained from Addgene. P561-luc-IRF3 firefly reporter was kindly provided by Xiaoxia Li

(Cleveland Clinic, Cleveland, OH). The pGL4.20(luc2/puro)-IFNβ firefly luciferase promoter reporter was a gift from Tilmann Bürckstümmer (Austrian Academy of Sciences, Vienna, Austria). pNF-κβ firefly luciferase and pRL-TK Renilla plasmids were obtained from ClonTech. Horseradish peroxidase-anti-FLAG (M2; F1804) and anti-VSV (P5D4; V5507) antibodies were obtained from Sigma. Anti-GEF-H1 phosphorylated at S885 (ab74156), anti-IRF3 (D83B9; 4302), anti-IRF3 phosphorylated at Ser396 (4D4G; 4947), anti-TBK1 (D1B4; 3504), anti-MAVS (3993), anti-STAT1 (9172), anti-STAT1 phosphorylated at Tyr701 (58D6; 9167), anti-IKKε (D61F9; 3416), anti-IκBα (L35A5; 4814), anti-p65 phosphorylated at S536 (93H1; 3033), anti-p65 (D14E12; 8242), anti-β-actin (8H10D10; 3700), and anti-PCNA (D3H8P; 13110) antibodies were purchased from Cell Signaling Technology. Anti-α-tubulin antibody (ab4074) was obtained from Abcam. Anti-GEF-H1 antibody (x1089p) was purchased from Exalpha Biologicals. Alexa Fluor 488 Phallodin was obtained from Invitrogen. Anti-influenza A/PR/8/34 nucleoprotein antibody was a gift from Adolfo García-Sastre (Mount Sinai School of Medicine, New York, NY). FITC-conjugated donkey anti-sheep IgG (H+L) (713-095-147) and Cy3-comjugated donkey anti-rabbit IgG (H+L) (711-165-152) antibodies were purchased from Jackson ImmunoResearch Laboratories.

Immunoprecipitation and immunoblotting

HEK293T cells were transfected with indicated plasmids using Lipofectamine 2000 (Invitrogen) according to the manufacturer's protocol. For the experiment of GEF-H1 and TBK1 interaction, HEK293T cells were first transfected with GEF-H1-VSV and TBK1-Flag plasmid by Lipofectamine 2000 for 24 h, then were treated with nocodazole (1 or 10 μM), forskolin (10 μM), or okadaic acid (1 nM) for 40 minutes followed by immunoprecipitation and immunoblotting. The preparation of cell total lysates for immunoprecipitation and immunoblotting has been described previously[7]. Nuclear and cytoplasmic extracts from bone marrow-derived macrophages were prepared according to published methods[41] with modifications: buffer A (10 mM HEPES, 1.5 mM $MgCl_2$, 10 mM KCl, 0.1 mM EDTA, 0.1 mM EGTA, 1 mM DTT, 0.3 mM Na_3VO_4) and buffer C (20 mM HEPES, 1.5 mM $MgCl_2$, 1 mM EDTA, 1 mM EGTA, 1 mM DTT, 0.3 mM Na_3VO_4, 0.4 M NaCl, 1 mM PMSF). Densitometry analysis of Immunoblots was done by ImageJ (NIH).

Viruses and viral infection

Influenza A virus (PR/8/1934), A/PR/8/1934 ΔNS1, A/PR/8/1934 NS1-GFP and anti-NP antibody were kindly provided by Adolfo García-Sastre (Mount Sinai School of Medicine, New York, NY). EMCV was purchased from ATCC. VSV was a gift from Charles Rice and Margaret MacDonald at The Rockefeller University. Bone marrow-derived macrophages from WT and *Arhgef2*$^{-/-}$ mice were infected with virus in DPBS with 1% FBS at indicated MOI for 1 h. Infection was continued for various times in the presence of serum-containing DMEM. For the *in vivo* influenza A/PR/8/1934 infection, *Arhgef2*$^{-/-}$ mice and their littermate controls were anesthetized and challenged with 20 μl (10 μl per nostril) of influenza A/PR/8/1934 suspension (10^3 pfu) intranasally.

Plaque assay

Supernatants from infected cells were used to measure viral titers by plaque assays. Monolayers of BHK-21 cells were used for VSV plaque assays. After 1 h of viral infection, BHK-21 cells were overlaid with 1.5% LE agarose for 1 day. The cells were then fixed with 7% formaldehyde followed by crystal violet staining. Plaques were counted to determine the titers.

Bacterial infection

Salmonella enterica serovar *typhimurium* strain SL1344 was used. Bacterial cultures were prepared by inoculating 10 ml of LB with 0.01 ml of a stationary phase culture, followed by a 16 h incubation at 37°C. Bone marrow derived macrophages were spininfected at moi=10 for 15 minutes at 750 rpm followed by incubation at 37°C for 45 minutes. Cells were washed twice before the addition of 100 μg/ml gentamicin in DMEM with 10 % FBS. 1 h after infection, macrophages were given fresh DMEM medium containing 10% FBS and 10 μg/ml gentamicin for the reminder of the experiment. For the determination of intracellular replication of *S. typhimurium*, cells were lysed in 1% Triton X-100 in PBS. Lysates were serially diluted in DMEM and plated on LB agar plates containing 100 μg/ml streptomycin for colony enumeration.

Gene expression analysis

Mouse bone marrow-derived macrophages and alveolar macrophages were isolated and treated as described above. Qiagen RNeasy kit was used for the extraction of RNA from all cell types examined and, after synthesis of cDNA with iScript cDNA synthesis kit (Bio-Rad), iQ SYBR Green Supermix kit (Bio-Rad) was used for real-time PCR (Bio-Rad CFX96 Real-Time PCR Detection System) according to the manufacturer's specifications. The value obtained for each gene was normalized to that of the *GAPDH* gene. Primers were as follows: IFN-β forward, 5′-ccctatggagatgacggaga-3′, and reverse, 5′-ctgtctgctggtggagttca-3′; IL-6 forward, 5′-ctgatgctggtgacaaccac-3′, and reverse, 5′-tccacgatttcccagagaac-3′; TNFα forward, 5′-tagccaggagggagaacaga-3′, and reverse, 5′-ttttctggagggagatgtgg-3′; GAPDH forward, 5′-aactttggcattgtggaagg-3′, and reverse, 5′-ggatgcagggatgatgttct-3′; Influenza NS1 forward, 5′-tcgagacagccacacgtgctggaaa-3′; Influenza NS1 reverse, 5′-aagagggcctgccactttctgcttg-3′; EMCV 2A-2B forward, 5′-aatgcccactacgctggt-3′; EMCV 2A-2B reverse, 5′-gtcgttcggcagtagggt-3′.

Measurement of cytokine production

Concentration of IFN-β in cell culture supernatants was measured using commercial ELISA kits (PBL interferon source) or Luminex assays (Affymetrix) according the manufacturers' instructions.

Luciferase assay

HEK293T cells were transfected with 50 ng of IFNβ, p561, or NF-κB firefly luciferase reporter and 0.5 ng of pRL-Renilla reporter together with expression plasmids by Lipofectamine 2000. For control experiments, empty pcDNA3.1 were utilized. Transfection of WT and *Arhgef2*$^{-/-}$ macrophages was carried out using Amaxa Mouse Macrophage

Nucleofector kits. Luciferase assays were performed 24 h post transfection using the Dual-Luciferase Reporter Assay System (Promega) according to the manufacturer's instructions.

Flow cytometry

Isolated cells from spleen and mesenteric lymph nodes were incubated in 10% donkey serum and Fc block for 20 minutes at 4°C and then stained with the following fluorescent-conjugated antibodies: APC-conjugated anti-CD11c (HL3; 550261), PE-conjugated anti-F4/80 (6F12; 552958), PE-conjugated anti-CD103 (M290; 557495), APC-Cy7-conjugated CD4 (GK1.5; 552051), PerCP-conjugated CD8 (53-6.7; 553036), FITC-conjugated anti-NK1.1 (PK136; 553164), and APC-conjugated a anti-CD19 (1D3; 550992). All antibodies were obtained from BD Pharmingen. Cells were analyzed on a FACSCalibur flow cytometer (BD Bioscience) and analyzed by FlowJo (Tree Star).

Confocal microscopy

WT or *Arhgef2*$^{-/-}$ bone marrow-derived macrophages were plated on 4-well chamber coverglass (Lab-Tek) and stimulated with poly(I:C)-Rhodamine or infected with influenza A/PR/8 NS1-GFP at indicated time periods. Live cells were imaged with a Nikon A1R-A1 confocal microscope. Image acquisition was carried out with NIS-Elements imaging software (Nikon) followed by analyses by Volocity (PerkinElmer). Immunofluorescence staining and imaging were performed as previously described[7].

Sampling BAL fluid and alveolar macrophages

Bronchoalveolar lavages were recovered by cannulation with 1000 μl of PBS after terminal exsanguination. To obtain alveolar macrophages, cells were washed and then enriched by centrifugation.

Histopathology analysis

To assess histological changes of lung following infection with influenza A/PR/8/1934 infection, anesthetized mice were exsanguinated via the abdominal aorta, and their lung tissues were fixed in 4% formaldehyde overnight at 4°C. The tissues were dehydrated by gradually soaking in alcohol and xylene and then embedded in paraffin. Specimens were cut into 5 μm sections and stained with Hamp;E. Lung sections were evaluated 'blinded' to sample identity and scored based on assessments of lung tissue destruction, epithelial cell layer damage, polymorphonuclear cell infiltration into the inflammation site, and alveolitis on a scale of 0-5 each parameters (0, none; 5 severe).

Statistical Analysis

GraphPad Prism was used for all statistical analysis. Total sample size was determined based on the previous studies with similar genetically modified mouse with comparable functional defects. All experiments were repeated at least three times. Statistical analysis was carried out by two-way analysis of variance (ANOVA) followed by Student's t-test. A P value < 0.05 was considered statistically significant.

Supplementary Material

Refer to Web version on PubMed Central for supplementary material.

ACKNOWLEDGMENTS

This work was supported by grants AI093588 (HCR), DK-068181 (HCR), DK-033506 (HCR), DK-043351 (HCR, CT) and DK-52510 (CT) from the National Institutes of Health

REFERENCES

1. Takeuchi O, Akira S. Pattern recognition receptors and inflammation. Cell. 2010; 140(6):805–820. [PubMed: 20303872]
2. Desmet CJ, Ishii KJ. Nucleic acid sensing at the interface between innate and adaptive immunity in vaccination. Nat Rev Immunol. 2012; 12(7):479–491. [PubMed: 22728526]
3. Merino-Gracia J, Garcia-Mayoral MF, Rodriguez-Crespo I. The association of viral proteins with host cell dynein components during virus infection. FEBS J. 2011; 278(17):2997–3011. [PubMed: 21777384]
4. Krendel M, Zenke FT, Bokoch GM. Nucleotide exchange factor GEF-H1 mediates cross-talk between microtubules and the actin cytoskeleton. Nat Cell Biol. 2002; 4(4):294–301. [PubMed: 11912491]
5. Meiri D, Marshall CB, Greeve MA, Kim B, Balan M, Suarez F, et al. Mechanistic insight into the microtubule and actin cytoskeleton coupling through dynein-dependent RhoGEF inhibition. Mol Cell. 2012; 45(5):642–655. [PubMed: 22405273]
6. Matsuzawa T, Kuwae A, Yoshida S, Sasakawa C, Abe A. Enteropathogenic Escherichia coli activates the RhoA signaling pathway via the stimulation of GEF-H1. EMBO J. 2004; 23(17):3570–3582. [PubMed: 15318166]
7. Fukazawa A, Alonso C, Kurachi K, Gupta S, Lesser CF, McCormick BA, et al. GEF-H1 mediated control of NOD1 dependent NF-kappaB activation by Shigella effectors. PLoS Pathog. 2008; 4(11):e1000228. [PubMed: 19043560]
8. Zhao Y, Alonso C, Ballester I, Song JH, Chang SY, Guleng B, et al. Control of NOD2 and Rip2-dependent innate immune activation by GEF-H1. Inflamm Bowel Dis. 2012; 18(4):603–612. [PubMed: 21887730]
9. Yoneyama M, Fujita T. RNA recognition and signal transduction by RIG-I-like receptors. Immunol Rev. 2009; 227(1):54–65. [PubMed: 19120475]
10. Lund JM, Alexopoulou L, Sato A, Karow M, Adams NC, Gale NW, et al. Recognition of single-stranded RNA viruses by Toll-like receptor 7. Proc Natl Acad Sci U S A. 2004; 101(15):5598–5603. [PubMed: 15034168]
11. Alexopoulou L, Holt AC, Medzhitov R, Flavell RA. Recognition of double-stranded RNA and activation of NF-kappaB by Toll-like receptor 3. Nature. 2001; 413(6857):732–738. [PubMed: 11607032]
12. Takeuchi O, Akira S. Innate immunity to virus infection. Immunol Rev. 2009; 227(1):75–86. [PubMed: 19120477]
13. Yoneyama M, Kikuchi M, Matsumoto K, Imaizumi T, Miyagishi M, Taira K, et al. Shared and unique functions of the DExD/H-box helicases RIG-I, MDA5, and LGP2 in antiviral innate immunity. J Immunol. 2005; 175(5):2851–2858. [PubMed: 16116171]
14. Zhang Z, Yuan B, Bao M, Lu N, Kim T, Liu YJ. The helicase DDX41 senses intracellular DNA mediated by the adaptor STING in dendritic cells. Nat Immunol. 2011; 12(10):959–965. [PubMed: 21892174]
15. Gitlin L, Barchet W, Gilfillan S, Cella M, Beutler B, Flavell RA, et al. Essential role of mda-5 in type I IFN responses to polyriboinosinic:polyribocytidylic acid and encephalomyocarditis picornavirus. Proc Natl Acad Sci U S A. 2006; 103(22):8459–8464. [PubMed: 16714379]

16. Kato H, Takeuchi O, Sato S, Yoneyama M, Yamamoto M, Matsui K, et al. Differential roles of MDA5 and RIG-I helicases in the recognition of RNA viruses. Nature. 2006; 441(7089):101–105. [PubMed: 16625202]
17. Kato H, Takeuchi O, Mikamo-Satoh E, Hirai R, Kawai T, Matsushita K, et al. Length-dependent recognition of double-stranded ribonucleic acids by retinoic acid-inducible gene-I and melanoma differentiation-associated gene 5. J Exp Med. 2008; 205(7):1601–1610. [PubMed: 18591409]
18. Hornung V, Ellegast J, Kim S, Brzozka K, Jung A, Kato H, et al. 5′-Triphosphate RNA is the ligand for RIG-I. Science. 2006; 314(5801):994–997. [PubMed: 17038590]
19. Pichlmair A, Schulz O, Tan CP, Naslund TI, Liljestrom P, Weber F, et al. RIG-I-mediated antiviral responses to single-stranded RNA bearing 5′-phosphates. Science. 2006; 314(5801):997–1001. [PubMed: 17038589]
20. Taniguchi T, Takaoka A. The interferon-alpha/beta system in antiviral responses: a multimodal machinery of gene regulation by the IRF family of transcription factors. Curr Opin Immunol. 2002; 14(1):111–116. [PubMed: 11790540]
21. Ishikawa H, Ma Z, Barber GN. STING regulates intracellular DNA-mediated, type I interferon-dependent innate immunity. Nature. 2009; 461(7265):788–792. [PubMed: 19776740]
22. Parvatiyar K, Zhang Z, Teles RM, Ouyang S, Jiang Y, Iyer SS, et al. The helicase DDX41 recognizes the bacterial secondary messengers cyclic di-GMP and cyclic di-AMP to activate a type I interferon immune response. Nat Immunol. 2012; 13(12):1155–1161. [PubMed: 23142775]
23. Fitzgerald KA, McWhirter SM, Faia KL, Rowe DC, Latz E, Golenbock DT, et al. IKKepsilon and TBK1 are essential components of the IRF3 signaling pathway. Nat Immunol. 2003; 4(5):491–496. [PubMed: 12692549]
24. Yang K, Shi H, Qi R, Sun S, Tang Y, Zhang B, et al. Hsp90 regulates activation of interferon regulatory factor 3 and TBK-1 stabilization in Sendai virus-infected cells. Mol Biol Cell. 2006; 17(3):1461–1471. [PubMed: 16394098]
25. Birkenfeld J, Nalbant P, Yoon SH, Bokoch GM. Cellular functions of GEF-H1, a microtubule-regulated Rho-GEF: is altered GEF-H1 activity a crucial determinant of disease pathogenesis? Trends Cell Biol. 2008; 18(5):210–219. [PubMed: 18394899]
26. Meiri D, Greeve MA, Brunet A, Finan D, Wells CD, LaRose J, et al. Modulation of Rho guanine exchange factor Lfc activity by protein kinase A-mediated phosphorylation. Mol Cell Biol. 2009; 29(21):5963–5973. [PubMed: 19667072]
27. Zenke FT, Krendel M, DerMardirossian C, King CC, Bohl BP, Bokoch GM. p21-activated kinase 1 phosphorylates and regulates 14-3-3 binding to GEF-H1, a microtubule-localized Rho exchange factor. J Biol Chem. 2004; 279(18):18392–18400. [PubMed: 14970201]
28. Garcia A, Cayla X, Sontag E. Protein phosphatase 2A: a definite player in viral and parasitic regulation. Microbes Infect. 2000; 2(4):401–407. [PubMed: 10817642]
29. Zhang Z, Yuan B, Lu N, Facchinetti V, Liu YJ. DHX9 pairs with IPS-1 to sense double-stranded RNA in myeloid dendritic cells. J Immunol. 2011; 187(9):4501–4508. [PubMed: 21957149]
30. Diebold SS, Kaisho T, Hemmi H, Akira S, Reis e, Sousa C. Innate antiviral responses by means of TLR7-mediated recognition of single-stranded RNA. Science. 2004; 303(5663):1529–1531. [PubMed: 14976261]
31. Garcia-Sastre A, Egorov A, Matassov D, Brandt S, Levy DE, Durbin JE, et al. Influenza A virus lacking the NS1 gene replicates in interferon-deficient systems. Virology. 1998; 252(2):324–330. [PubMed: 9878611]
32. Manicassamy B, Manicassamy S, Belicha-Villanueva A, Pisanelli G, Pulendran B, Garcia-Sastre A. Analysis of in vivo dynamics of influenza virus infection in mice using a GFP reporter virus. Proc Natl Acad Sci U S A. 2010; 107(25):11531–11536. [PubMed: 20534532]
33. Georgel P, Jiang Z, Kunz S, Janssen E, Mols J, Hoebe K, et al. Vesicular stomatitis virus glycoprotein G activates a specific antiviral Toll-like receptor 4-dependent pathway. Virology. 2007; 362(2):304–313. [PubMed: 17292937]
34. Kumar H, Kawai T, Kato H, Sato S, Takahashi K, Coban C, et al. Essential role of IPS-1 in innate immune responses against RNA viruses. J Exp Med. 2006; 203(7):1795–1803. [PubMed: 16785313]

35. Arpaia N, Godec J, Lau L, Sivick KE, McLaughlin LM, Jones MB, et al. TLR signaling is required for Salmonella typhimurium virulence. Cell. 2011; 144(5):675–688. [PubMed: 21376231]
36. Wittmann T, Waterman-Storer CM. Cell motility: can Rho GTPases and microtubules point the way? J Cell Sci. 2001; 114(Pt 21):3795–3803. [PubMed: 11719546]
37. Misawa T, Takahama M, Kozaki T, Lee H, Zou J, Saitoh T, et al. Microtubule-driven spatial arrangement of mitochondria promotes activation of the NLRP3 inflammasome. Nat Immunol. 2013; 14(5):454–460. [PubMed: 23502856]
38. Ohman T, Rintahaka J, Kalkkinen N, Matikainen S, Nyman TA. Actin and RIG-I/MAVS signaling components translocate to mitochondria upon influenza A virus infection of human primary macrophages. J Immunol. 2009; 182(9):5682–5692. [PubMed: 19380815]
39. Palazzo AF, Cook TA, Alberts AS, Gundersen GG. mDia mediates Rho-regulated formation and orientation of stable microtubules. Nat Cell Biol. 2001; 3(8):723–729. [PubMed: 11483957]
40. Minin AA, Kulik AV, Gyoeva FK, Li Y, Goshima G, Gelfand VI. Regulation of mitochondria distribution by RhoA and formins. J Cell Sci. 2006; 119(Pt 4):659–670. [PubMed: 16434478]
41. Perry AK, Chow EK, Goodnough JB, Yeh WC, Cheng G. Differential requirement for TANK-binding kinase-1 in type I interferon responses to toll-like receptor activation and viral infection. J Exp Med. 2004; 199(12):1651–1658. [PubMed: 15210743]
42. Sakaguchi S, Negishi H, Asagiri M, Nakajima C, Mizutani T, Takaoka A, et al. Essential role of IRF-3 in lipopolysaccharide-induced interferon-beta gene expression and endotoxin shock. Biochem Biophys Res Commun. 2003; 306(4):860–866. [PubMed: 12821121]
43. Aksoy E, Vanden Berghe W, Detienne S, Amraoui Z, Fitzgerald KA, Haegeman G, et al. Inhibition of phosphoinositide 3-kinase enhances TRIF-dependent NF-kappa B activation and IFN-beta synthesis downstream of Toll-like receptor 3 and 4. Eur J Immunol. 2005; 35(7):2200–2209. [PubMed: 15940673]
44. Honda K, Yanai H, Takaoka A, Taniguchi T. Regulation of the type I IFN induction: a current view. Int Immunol. 2005; 17(11):1367–1378. [PubMed: 16214811]
45. Peters KL, Smith HL, Stark GR, Sen GC. IRF-3-dependent, NFkappa B- and JNK-independent activation of the 561 and IFN-beta genes in response to double-stranded RNA. Proc Natl Acad Sci U S A. 2002; 99(9):6322–6327. [PubMed: 11972054]
46. Wang X, Hussain S, Wang EJ, Li MO, Garcia-Sastre A, Beg AA. Lack of essential role of NF-kappa B p50, RelA, and cRel subunits in virus-induced type 1 IFN expression. J Immunol. 2007; 178(11):6770–6776. [PubMed: 17513724]
47. Akira S, Uematsu S, Takeuchi O. Pathogen recognition and innate immunity. Cell. 2006; 124(4): 783–801. [PubMed: 16497588]
48. Hale BG, Randall RE, Ortin J, Jackson D. The multifunctional NS1 protein of influenza A viruses. J Gen Virol. 2008; 89(Pt 10):2359–2376. [PubMed: 18796704]
49. Hengge R. Principles of c-di-GMP signalling in bacteria. Nat Rev Microbiol. 2009; 7(4):263–273. [PubMed: 19287449]
50. Paludan SR, Bowie AG, Horan KA, Fitzgerald KA. Recognition of herpesviruses by the innate immune system. Nat Rev Immunol. 2011; 11(2):143–154. [PubMed: 21267015]

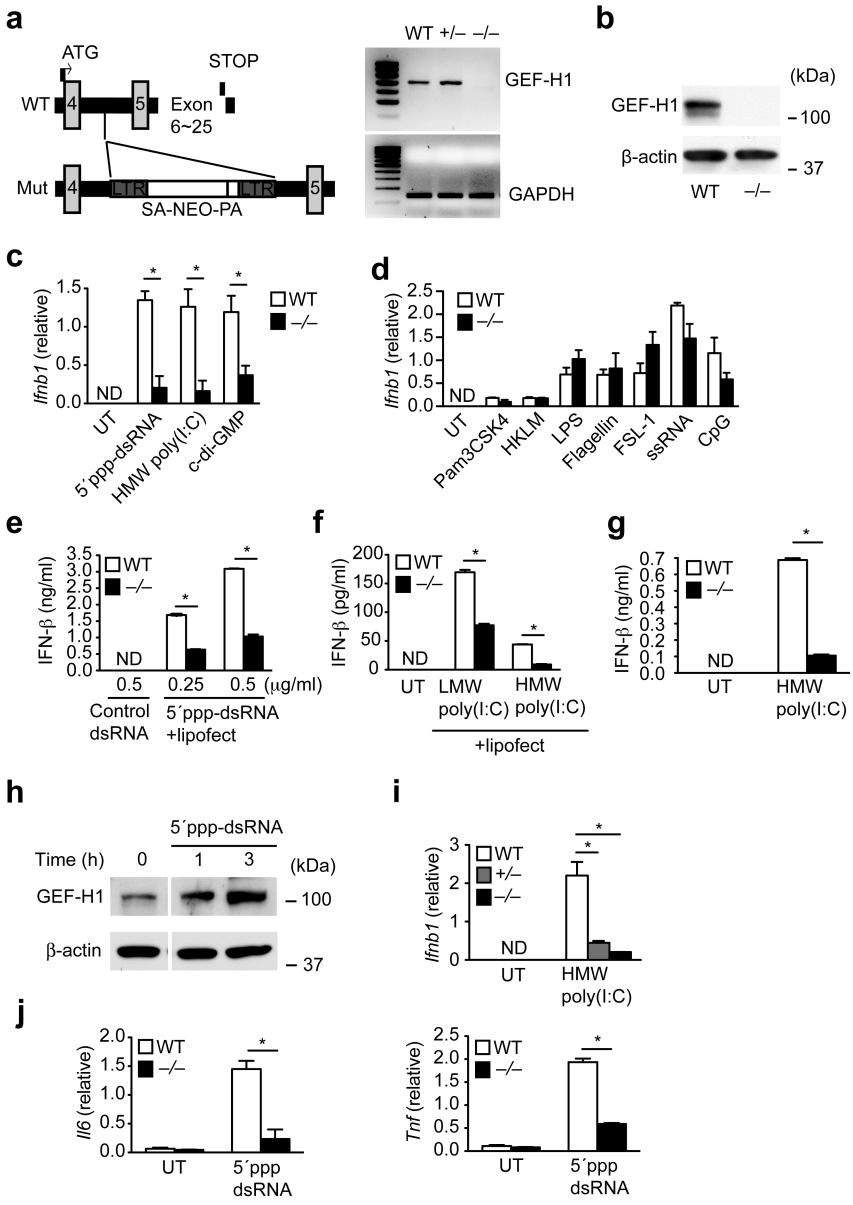

Figure 1.

GEF-H1 is essential for RLR-mediated IFN-β production. (**a**) Schematic diagram of the gene-trap vector and its site of insertion into *Arhgef2* gene. GEF-H1 mRNA expression in wild-type (WT), *Arhgef2* heterozygous (+/-), and *Arhgef2* homozygous (−/−) mice was determined by RT-PCR. (**b**) Immunoblot analysis of GEF-H1 expression in WT and *Arhgef2*$^{-/-}$ macrophages. (**c**, **d**) Quantitative RT-PCR analysis of *Ifnb1* mRNA expression in WT and *Arhgef2*$^{-/-}$ macrophages incubated for 16 h with transfected (**c**) 5′ppp-dsRNA (0.5 μg/ml), HMW poly(I:C) (0.5 μg/ml) or c-di-GMP (10 μg/ml) and (**d**) Pam3CSK4 (1 μg/ml), HKLM (10^8 cells/ml), LPS (0.2 μg/ml), Flagellin (1 μg/ml), FSL-1 (1 μg/ml), ssRNA (1 μg/ml) complexed with Lipofectamine (lipofect), and CpG ODN1826 (5 μM) complexed with Lipofectamine. (**e**-**g**) IFN-β secretion by WT and *Arhgef2*$^{-/-}$ macrophages in the presence of 5′ppp-dsRNA, LMW poly(I:C) or HMW poly(I:C) (0.5 μg/ml) complexed with

or without Lipofectamine for 24 h. (**h**) Immunoblot analysis of GEF-H1 expression in WT macrophages treated with transfected 5′ppp-dsRNA (0.5 μg/ml) for 1 or 3 h. (**i**) Quantitative RT-PCR analysis of *Ifnb1* mRNA expression in WT, *Arhgef2*$^{+/-}$ or *Arhgef2*$^{-/-}$ macrophages in the presence of HMW poly(I:C) (0.5 μg/ml) for 24 h. (**j**) Quantitative RT-PCR analysis of *Il6* and *Tnf* mRNA expression in WT and *Arhgef2*$^{-/-}$ macrophages incubated for 24 h with transfected 5′ppp-dsRNA (0.5 μg/ml). Results are presented relative to the expression of GAPDH. UT, untreated. ND, not detectable. **, $P < 0.01$ (Student's t-test). Data are from one experiment representative of three independent experiments. Error bars indicate mean ± SD.

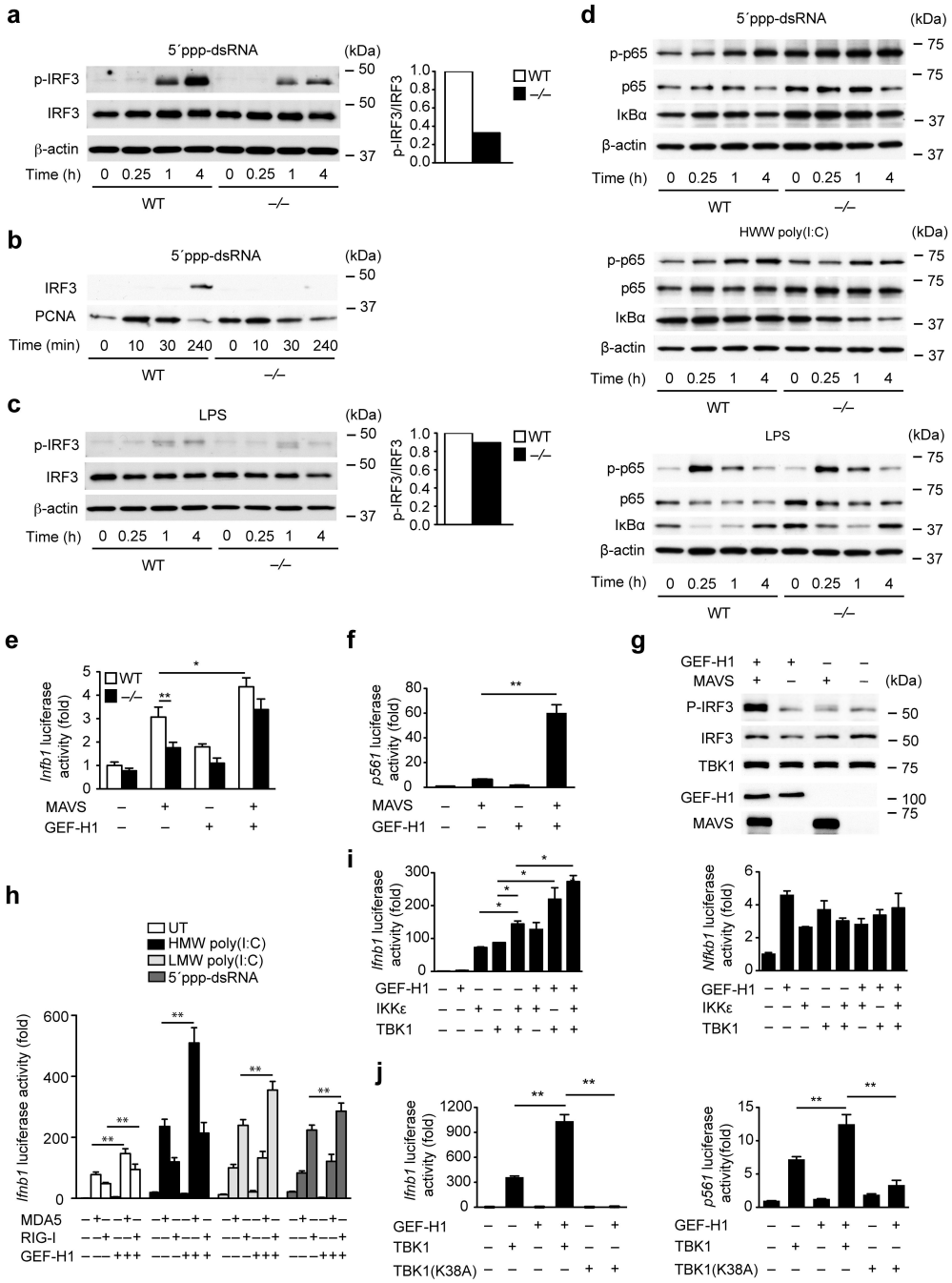

Figure 2.

GEF-H1 enhances TBK1-dependent IRF3 activation. (**a**) IRF3 phosphorylation and expression in cytoplasmic protein fractions of WT and *Arhgef2*$^{-/-}$ macrophages in response to transfected 0.5 μg/ml 5′ppp-dsRNA. (**b**) IRF3 expression in protein extractions from nuclei of WT and *Arhgef2*$^{-/-}$ macrophages in response to transfected 0.5 μg/ml 5′ppp-dsRNA. (**c**) Immunoblots of IRF3 phosphorylation in WT and *Arhgef2*$^{-/-}$ macrophages in the presence of LPS (0.2 μg/ml). β-actin and PCNA served as loading controls. Bar graphs represent densitometry analysis of phosphorylated IRF3 relative to IRF3 expression at 4 h.

(**d**) Immunoblot analysis of IκBα expression and p65 phosphorylation at S536 in WT and *Arhgef2*$^{-/-}$ macrophages incubated with transfected 0.5 μg/ml 5′ppp-dsRNA, HMW poly(I:C), or 0.2 μg/ml LPS. (**e**) *Ifnb1* promoter activation 24 h after transfection of WT or *Arhgef2*$^{-/-}$ macrophages with combinations of MAVS and GEF-H1 plasmids. (**f**) Assessment of MAVS and/or GEF-H1-mediated p561 luciferase reporter activation in HEK293T cells 24 h after transfection. (**g**) Immunoblot analysis of IRF3 phosphorylation in MAVS and/or GEF-H1-transfected HEK293T cells. **(h**) *Ifnb1* promoter activation in HEK293T cells expressing GEF-H1 and Mda5 or RIG-I in response to HMW poly(I:C), LMW poly(I:C) or 5′ppp-dsRNA stimulation for 24 h. (**i**) GEF-H1 and TBK1 or IKKε-mediated *Ifnb1* and *Nfkb1* promoter activation in HEK293T cells 24 h after transfection. (**j**) *Ifnb1* and p561 luciferase reporter activation 24 h after transfection of HEK293T cells with combinations of GEF-H1, TBK1 or TBK1 kinase-inactive (K38A) mutant plasmids. Data presented are from one experiment representative of three independent experiments and represented as fold induction relative to the reporter-only control and reflect mean ± SD. *, $P < 0.05$; **, $P < 0.01$ (Student's t-test).

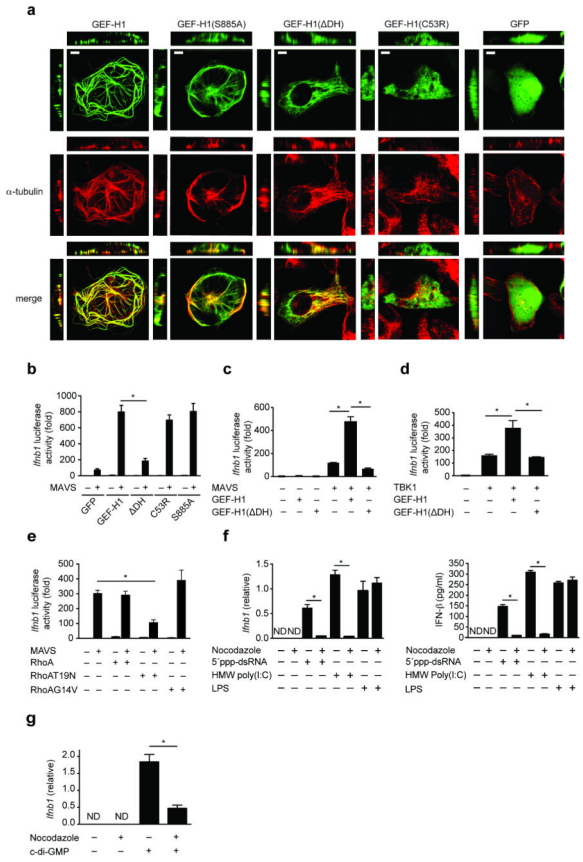

Figure 3.

GEF-H1 controls microtubule-dependent induction of IFN-β expression. (**a**) Confocal microscopy of COS-7 cells expressing GFP-tagged GEF-H1, GEF-H1 (S885A), GEF-H1 (ΔDH), and GEF-H1 (C53R). Scale bar, 10μm. (**b**) *Ifnb1* promoter activation by MAVS in HEK293T cells transfected with GFP-tagged GEF-H1, GEF-H1 (ΔDH), GEF-H1 (C53R) and GEF-H1 (S885A). (**c, d**) *Ifnb1* promoter activation by MAVS (**c**) or TBK1 (**d**) in HEK293T cells in the presence of GEF-H1 or GEF-H1 (ΔDH). (**e**) *Ifnb1* promoter activation by MAVS in HEK293T cells 24 h after transfection of RhoA, RhoA dominant negative variant (RhoAT19N), or constitutive variant (RhoAG14V) plasmids. Data are represented as fold induction relative to the reporter-only control. (**f**) Quantitative RT-PCR analysis of *Ifnb1* mRNA expression and IFN-β secretion in nocodazole-treated WT macrophages in the presence of 0.5 μg/ml transfected 5′ppp-dsRNA, HMW poly(I:C), or 0.2 μg/ml LPS for 24 h. (**g**) Quantitative RT-PCR analysis of *Ifnb1* mRNA expression in nocodazole-treated WT macrophages in the presence of transfected c-di-GMP (10 μg/ml) for 24 h. Results are presented relative to the expression of GAPDH. ND, not detectable. Data are from one experiment representative of three independent experiments and reflect mean ± SD. *, $P < 0.01$ (Student's t-test).

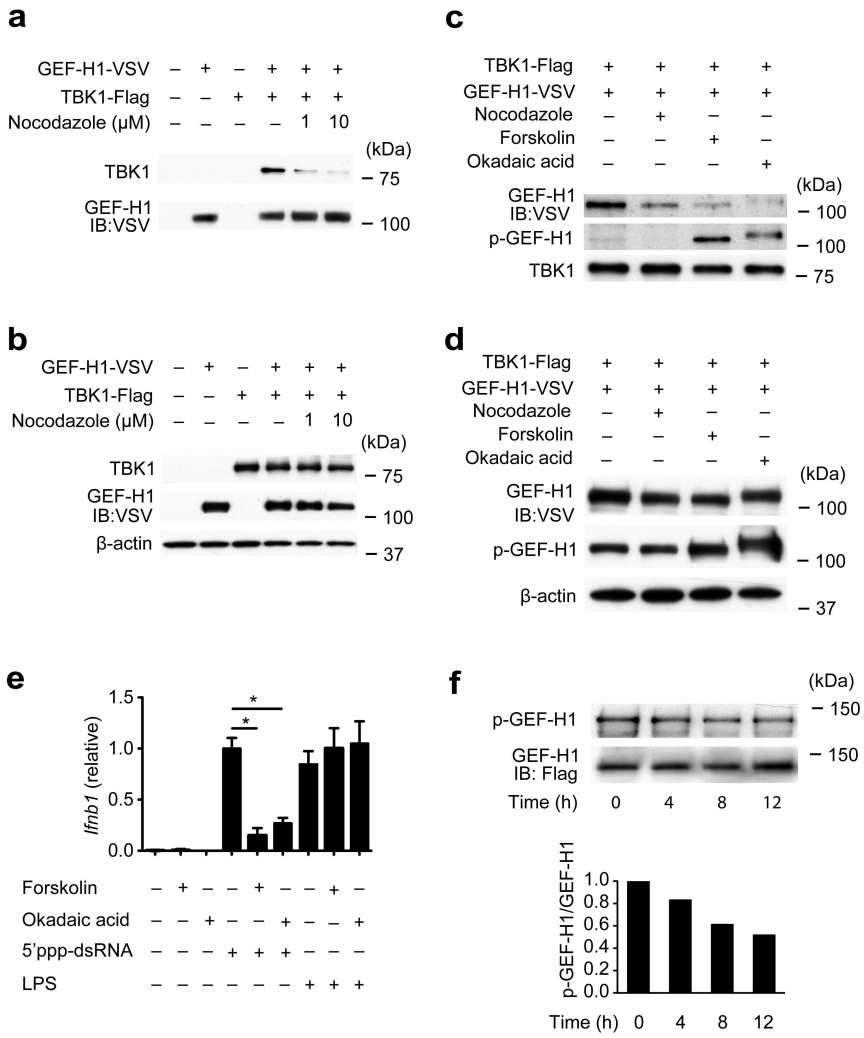

Figure 4 Polarized microtubules are required for the activation of GEF-H1 and interaction with TBK1. (**a**) Immunoprecipitation (IP) with anti-GEF-H1 and immunoblot (IB) for TBK1-Flag or GEF-H1-VSV expressed in HEK293T cells in the absence or presence of nocodazole for 40 minutes. (**b**) IB analysis of cell lysates utilized for the IP in panel a. (**c**) IP with anti TBK1 and IB detection of GEF-H1-VSV and GEF-H1 phosphorylated at Serine 885 with specific antibodies in HEK293T cells in the presence of nocodazole (10 μM), forskolin (10 μM), or okadaic acid (1 nM) for 40 minutes. (**d**) IB analysis of cell lysates utilized for IP in panel c. (**e**) Quantitative RT-PCR analysis of *Ifnb1* mRNA expression in 10 μM forskolin or 1 nM okadaic acid-treated WT macrophages in the presence of 0.5 μg/ml 5′ppp-dsRNA complexed with Lipofectamine, or 0.2 μg/ml LPS for 24 h. Results are represented relative to the expression of GAPDH and reflect mean ± SD. **, $P < 0.01$ (Student's t-test). (**f**) IP with anti-Flag and IB detection of GEF-H1 S885 phosphorylation in COS-7 cells after infection with NS1-deficient influenza A/PR/8/34. Bar graph represents densitometry analysis of phosphorylated GEF-H1 relative to GEF-H1 expression. Data are from one experiment representative of three independent experiments.

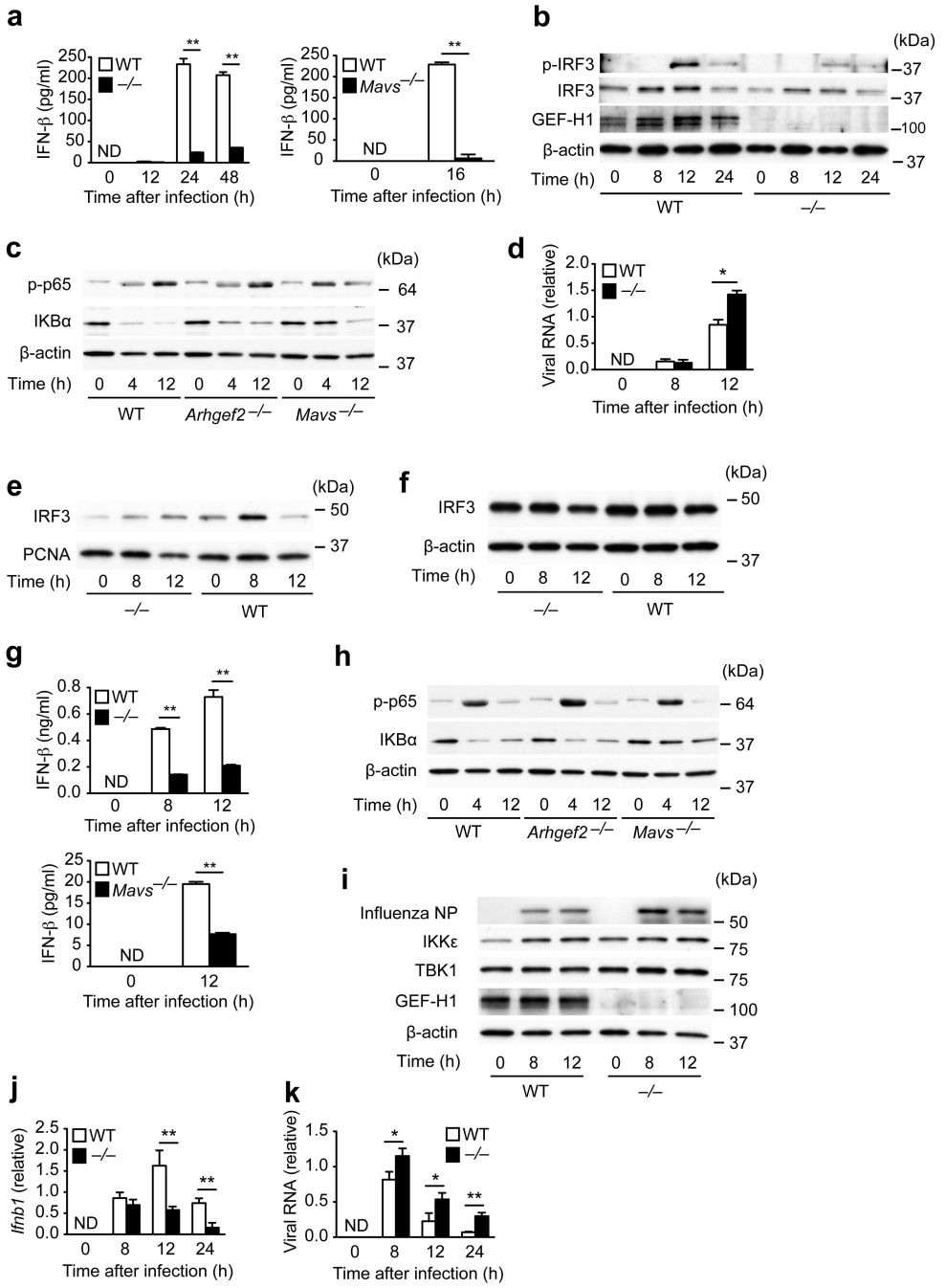

Figure 5.

GEF-H1 mediates host defenses against ssRNA viruses. **(a)** IFN-β secretion by EMCV-infected (MOI=0.1) WT, *Arhgef2*$^{-/-}$, and *Mavs*$^{-/-}$ macrophages. (**b**) Immunoblot analysis of IRF3 phosphorylation in WT and *Arhgef2*$^{-/-}$ macrophages after EMCV infection (MOI=0.1). **(c)** Immunoblot analysis of IκBα expression and phosphorylation of p65 at S536 in WT, *Arhgef2*$^{-/-}$ and *Mavs*$^{-/-}$ macrophages infected with EMCV (MOI=0.1). **(d)** Quantitative RT-PCR analysis of EMCV non-structural protein 2A and 2B mRNA in EMCV-infected (MOI=1) WT or *Arhgef2*$^{-/-}$ macrophages. (**e**) IRF3 expression in the

nuclear and (**f**) cytoplasmic protein fractions of WT and *Arhgef2*$^{-/-}$ macrophages infected with influenza A lacking the nonstructural protein NS1 gene (A/PR/8 ΔNS1) (MOI=1). (**g**) IFN-β expression in the supernatants of macrophages from WT, *Arhgef2*$^{-/-}$ and *Mavs*$^{-/-}$ mice after influenza A/PR/8 ΔNS1 infection (MOI=0.1). **(h)** Immunoblot analysis of IκBα expression and phosphorylation of p65 at S536 in WT, *Arhgef2*$^{-/-}$ and *Mavs*$^{-/-}$ macrophages infected with A/PR/8 ΔNS1 (MOI=0.1). (**i**) Immunoblot analysis of TBK1, IKKε expression and the presence of A/PR/8 nucleoprotein (NP) in A/PR/8 ΔNS1-infected WT and *Arhgef2*$^{-/-}$ macrophages (MOI=0.1). **(j, k)** Quantitative RT-PCR analysis of *Ifnb1* (**j**) or NS1 (**k**) mRNA in WT or *Arhgef2*$^{-/-}$ macrophages after influenza A/PR/8 infection (MOI=1). (**d**, **j**, **k**) Results are represented relative to the expression of GAPDH. ND, not detectable. Data are from one experiment representative of three independent experiments and reflect mean ± SD. *, $P < 0.05$; **, $P < 0.01$ (Student's t-test).

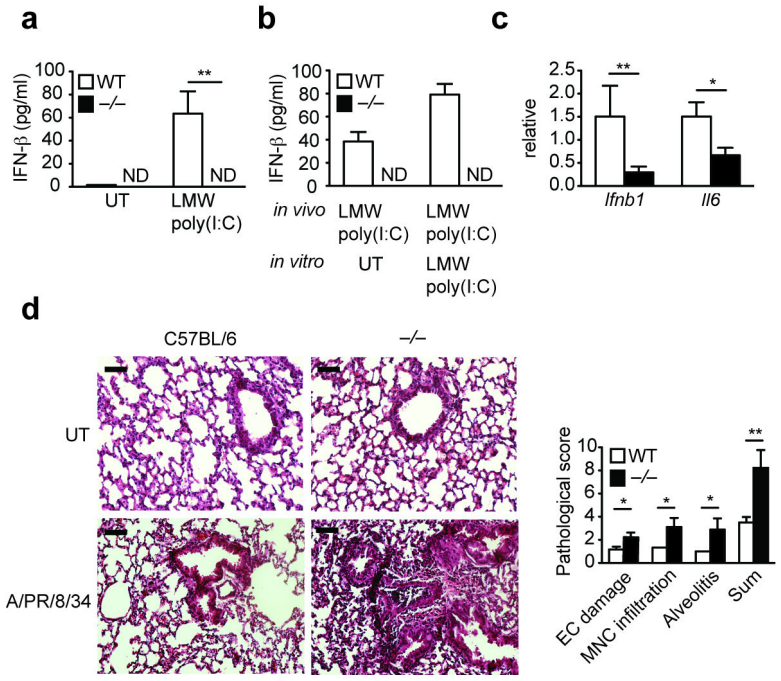

Figure 6.

GEF-H1 is required for the control of influenza A infection. **(a)** IFN-β secretion in bronchoalveolar lavage (BAL) fluid in WT and *Arhgef2*$^{-/-}$ mice (*n*=3 per group) 6 h post intranasal administration of LMW poly(I:C). **(b)** IFN-β secretion after 0.5 μg/ml LMW poly(I:C) restimulation for 24 h of alveolar macrophages isolated from LMW poly(I:C)-challenged WT or *Arhgef2*$^{-/-}$ mice. (**c**) Quantitative RT-PCR analysis of *Ifnb1* and *Il6* mRNA in alveolar macrophages from WT and *Arhgef2*$^{-/-}$ mice (*n*=3 in each group) 4 days after influenza A/PR/8 infection. (**d**) Haematoxylin and eosin staining of WT and *Arhgef2*$^{-/-}$ lungs, 4 days post influenza A/PR/8 infection (n=3 per group). Scale bar indicates 0.2 μm. The bar graph represents pathological scores. Data are from one experiment representative of three independent experiments. ND, not detectable. *, $P < 0.05$; **, $P < 0.01$ (Student's t-test). Error bars indicate mean ± SD.